

Research Article

Modelling and Simulation of Existing Geothermal Power Plant: A Case Study of Darajat Geothermal Power Plant

K. F. A. Sukra¹, D. I. Permana^{2*}, W. Adriansyah³

¹Research Center for Transportation Technology, National Research and Innovation Agency, South Tangerang, 15314, Indonesia

²Doctoral School of Mechanical Engineering, Hungarian University of Agriculture and Life Science, 2100 Godollo, Hungary

²Department of Mechanical Engineering, Institut Teknologi Nasional Bandung, 40124 Bandung, Indonesia

³Thermodynamic Laboratories, 3rd floor PAU Building, Institut Teknologi Bandung, 40116 Bandung, Indonesia
E-mails: ¹kurnia.fajar.adhi.sukra@brin.go.id , ^{2*}dicky91permana@itenas.ac.id , ³willy.adriansyah@gmail.com

Received 19 May 2022, Revised 27 January 2023, Accepted 26 February 2023

Abstract

The electrical energy needs grow every year, increasing awareness and use of renewable energy even higher. Geothermal power plants (GPP) are even ogled as a renewable energy source that has a lot of potential worldwide. Technology for GPP continues to evolve. However, tools for analyzing a system of GPP are still inadequate. In this study, a simple analysis tool was designed. The usefulness of this analysis tool is to be able to know the state of the GPP works. This tool will help simulate the conditions that may occur in the plant system. The simulation results will also be known operating conditions that may occur, so the operator can determine what should be done if things happen. Modeling started using Microsoft Excel, which has been equipped with thermodynamic properties. Modeling includes turbine, condenser, cooling tower, and extraction systems non-condensable gas. After validated, the model run simulation in variations that may occur such as decline in the condition of the condenser and cooling tower and environmental conditions, represented by relative humidity. The simulation with variation of condition will decrease the power generated from turbine 3 – 5%.

Keywords: Geothermal energy; design; simulation; power loss; environmental relative humidity.

1. Introduction

The world's energy needs are increasing daily along with the increase in the world's population, including in every sector in Indonesia as shown in the Figure 1. PT PLN, as the actor in the energy supply policy in Indonesia, issued a policy to electrify areas spread across Indonesia. Renewable energy sources will be used, such as solar, wind, water, biomass, geothermal, and non-renewable energy sources, such as coal, oil, and natural gas [1,2].

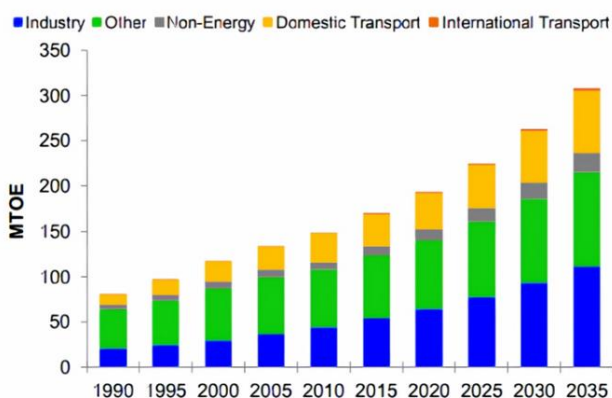


Figure 1. Indonesia's energy sector need [3] (Figure is in color in the on-line version of the paper).

However, the energy sources available in Indonesia are very diverse and quite abundant. Technology to process energy sources that will run out is already quite advanced and Table, but renewable energy now needs to be further developed so that there is no dependence on non-renewable energy sources. In line with this, the government through the directorate of Energy and Mineral Resources in the field of Renewable Energy (EBTKE) has also made a policy targeting the development of 23% renewable energy by 2025 [2].

Geothermal technology has long been developed worldwide and is considered one of the most reliable and provide a clean source of energy [4], especially in Indonesia, with about 29,164 MWe potential and only around 1341 MW is installed [5]. Geothermal energy uses heat energy stored in the earth, which is now expected to be clean renewable energy and can be used for various purposes such as heating district [6,7], agriculture [8,9], and energy generation [10–14]. However, the geothermal power plant (GPP) is quite sensitive to changes in air conditions because the working fluid is cooled using ambient air. When there is a change in environmental conditions, there will be a change in the power generated by the turbine. Michaelides [15] has conducted a study of the effect of ambient temperature fluctuation on the performance of GPP and the result is temperature of the GPP changes result in more than 20% of

power fluctuations. Kahraman et al [16] conduct a thermodynamic and thermo-economic analysis of air-cooled GPP and determined the effect of ambient temperature variation to GPP performance. While Sohel [17] changes the outlet temperature of the condenser with the ambient temperature, vaporized equilibrium pressure and temperature will be change. Lastly Rudiyanto et al [18] conducted a study case in Kamojang GPP in Indonesia, where he varies of ambient temperature from 17 to 20 °C.

Moreover, the literature study about ambient temperature in geothermal research is mostly related to secondary application such as binary cycle [19,20], Kalina cycle [21,22], organic Rankine cycle (ORC) and hybrid cycle [23,24].

From the available literature review[15,25–27], few authors study modeling from existing geothermal plants and simulating variables from ambient temperature with the resulting GPP performance. The lack of tools for quick, simple, and comprehensive analysis and simulation of a geothermal power generation system makes it difficult to carry out a basic analysis. The tool is needed to carry out initial analysis and possible steps to be taken if there is a change or deviation in operating conditions. The tool will make it easier for operators and users to predict changes in the generating system to some changes in environmental conditions. In this study, the authors conduct research in the form of making a tool to analyze the performance of a geothermal generating system so that it will be easier to make decisions if there is a change in circumstances from what has been determined and how to deal with it.

2. Darajat Geothermal Power Plant

The Darajat GPP is about 22 kilometers west of Garut, West Java. This geothermal region is roughly 10 kilometers southwest of the Kamojang geothermal field. Darajat is comparable to Kamojang in that it has a vapor-dominated reservoir. In this regard, these two reservoirs differ from Indonesia's more frequent geothermal water-dominated reservoir. The Darajat geothermal power plant has three units that generate a total of 270 MW. Darajat Unit I, which began operations in 2000, produces 55 MW; Darajat Unit II, which began construction in 2004 and began operations in 2007, produces 95 MW; and Darajat Unit III produces 121 MW.

Chevron owns Darajat and Gunung Salak before to the acquisition of Star Energy and Indonesia Power. Chevron is the world's largest geothermal producer, with 1273 MW capacity, and it created almost 27% of global geothermal power [32] Darajat generates energy using a dry-steam power plant due to its vapor-dominated reservoir. Steam from the reservoir rises to the surface and passes through a pressure regulator valve, which maintains a constant pressure. The steam travels into the scrubber through this valve, which enhances its quality by removing moisture. Dry steam pours into a turbine, spinning the turbine blade. The spinning of the turbine is what allows the generator to generate power. To keep the system running, steam from the exhaust turbine goes into the condenser.

We choose Darajat GPP as case study due to simplicity of the system. We would like to model simple analysis tool to help the operator know the condition of their GPP. The Darajat GPP still active as base load supply for Java, Madura, and Bali power transmission and one of the biggest renewable power plants in Java Island.

3. Methods

The implementation of this tool begins with obtaining operating data of the GPP system which can be used for modelling and validating the model that has been made. Furthermore, modelling is carried out for each equipment and merging the equipment into a single generating system. The modelled equipment includes turbines, condensers, cooling towers, and non-condensable gas extraction systems.

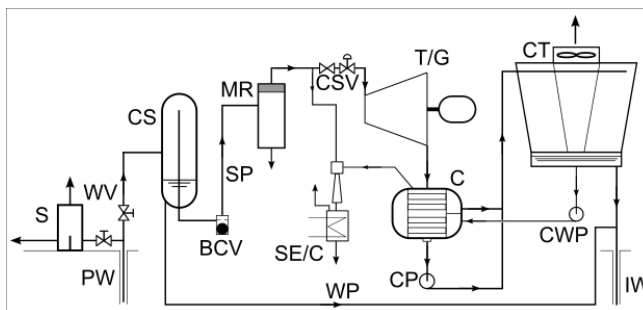


Figure 2. GPP schematic diagram [28].

Figure 22 and Figure 33 shows the scheme of the GPP system to be used as well as the Ts diagram of the geothermal power plant process. PW is a production well where water vapor is obtained and will be used as a working fluid. WV is valve while S is silencer. CS is a cyclone separator that separate the vapor phase and liquid phase so that only pure steam enters the flow from the separator to the MR, mist remover, to get the steam as clean as possible to flow into the turbine. SE/C is a steam ejector/condenser that removes non-condensable gas in the condenser, C, which works using part of the steam for the turbine, T. CP and CWP are pumps for circulation between the condenser and cooling tower, CT. Finally, the water will be put back into the bowels of the earth through IW, injection well.

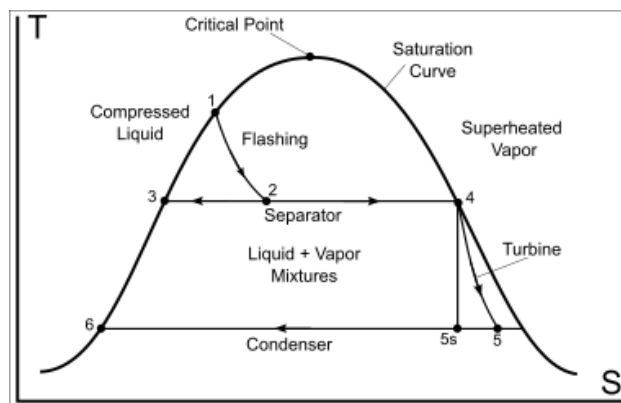


Figure 3. GPP T-s diagram [28].

3.1 Steam Turbine Model

This turbine modelling includes turbine efficiency factor ($\eta_{Turbine}$). The efficiency is obtained from the calculation of the operating conditions that are already running. From the operating data, the enthalpy value of the steam leaving the turbine can be determined. From this enthalpy value, turbine efficiency can be calculated under these conditions [29]. Turbine efficiency is used as a parameter in the next turbine modelling. Equation (1) is used for turbine modelling.

$$\eta_{Turbine} = \frac{h_4 - h_5}{h_4 - h_{5s}} \quad (1)$$

$$\dot{W}_{Turbine} = \dot{m}_4(h_4 - h_5) = x_2 \dot{m}_1(h_4 - h_5) \quad (2)$$

3.2 Condenser Model

The steam from the turbine expansion will go directly to the condenser. The steam is cooled and then injected into the bowels of the earth. The condenser used in this model is a direct contact type, where the steam coming out of the turbine is directly in contact with the cooling fluid in the form of water which is sprayed on the top of the condenser. The cooling tower cools the water leaving the condenser. Figure 4 shows the condenser modelling system used.

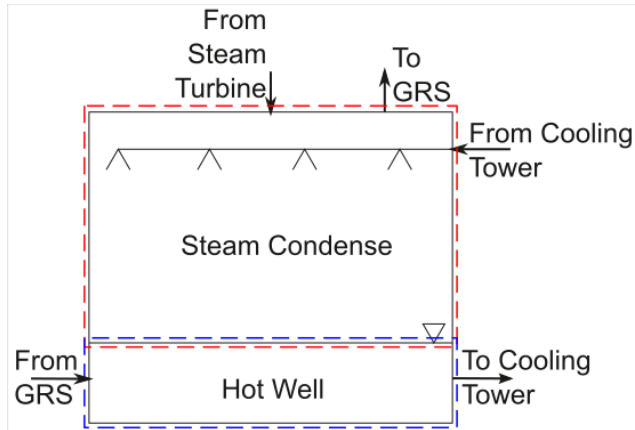


Figure 4. Condenser model.

The condenser system used is direct contact type. The condenser is modelled in the direct contact heat transfer process section and the hot well section. Figure 44 shows the division of the condenser modelling process; the condensation section is modelled by the direct contact process between steam from the turbine and water from the cooling tower in a saturated condition so that the final condition is water in a saturated liquid condition. Meanwhile, in the hot well section, the bottom part is modelled by mixing conditions between water from the gas removal system (GRS) and saturated liquid conditions because of cooling steam and water to cool so that an equilibrium condition of water temperature will be obtained which will flow into the cooling tower. The cooling water requirement can be calculated using the equation below.

$$\dot{m}_{cw} = x_2 \dot{m}_1 \left| \frac{h_5 - h_6}{c_p(T_6 - T_{cw})} \right|, \quad (3)$$

The pressure in the condenser is usually made as vacuum as possible so that the power generated by the turbine can be as large as possible. In steam from geothermal heat, there is usually gas that cannot be condensed and will collect in the condenser, which will impact the pressure in the condenser [29,30]. To prevent this, a GRS system is needed to remove the gas.

3.3 Cooling Tower Model

The next modelled component is the cooling tower. The cooling tower serves to prepare cooling water for the condenser by cooling the water from the condenser using ambient air. The ability of the cooling tower is very dependent on environmental conditions; changes in environmental conditions will cause the cooling water to be inappropriate and may reduce the power produced by the turbine. Figure 55 is a modelling form for a cooling tower system.

The cooling tower system is modelled into two parts. The fogging section and the hot well section. At the top is the cooling water from the condenser, which is atomized and mixed with the ambient air. The cooled water is partly carried away by the environmental air and partly down to the hot well. The ambient air that cools the water from the condenser will increase in humidity, so that the air leaving the cooling tower will become saturated with water. Increasing the moisture level in the air will reduce the cooling effectiveness of the cooling tower.

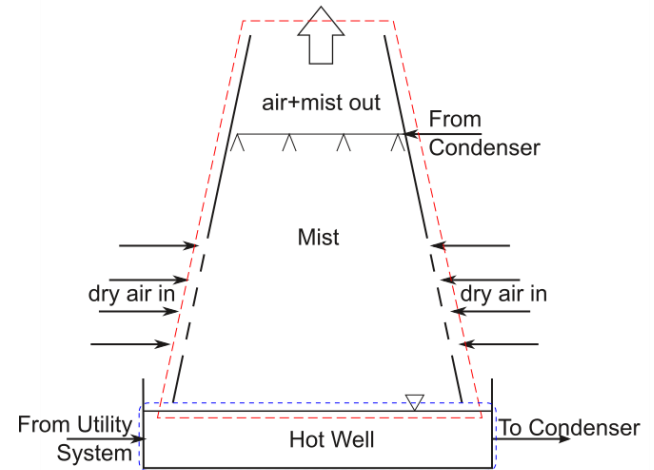


Figure 5. Cooling tower model.

Figure 6 shows a schematic diagram of a cooling tower. Using the principle of energy conservation, we get the equation (4); the heat removed will be equal the heat absorbed by the working fluid. The water coming from the steam condensate will be cooled by the outside air, but some of the water will be carried away until the air condition comes out to reach its saturation point. Water not carried will fall into the blow-down or reservoir and flow to the condenser.

$$\dot{m}_7 h_7 - \dot{m}_8 h_8 = \dot{m}_d h_d - \dot{m}_a h_a + \dot{m}_b h_b, \quad (4)$$

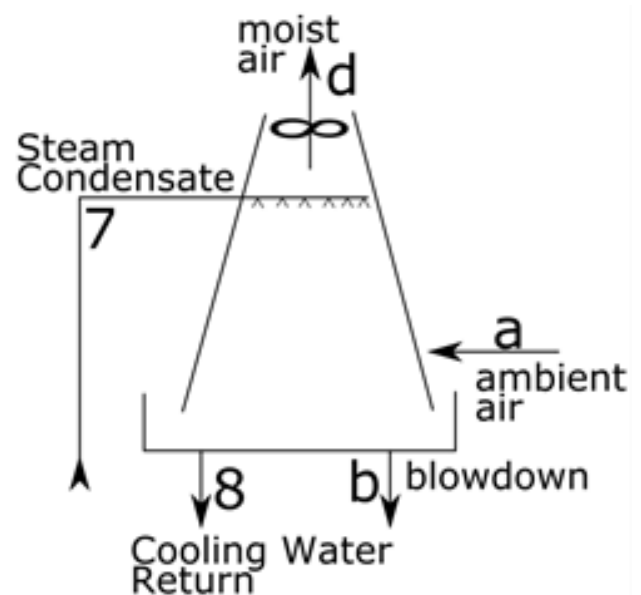


Figure 6. Simple schematic of cooling tower [29].

3.4 Gas Removal System

The GRS configuration consists of an ejector, inter condenser, liquid ring vacuum pump (LRVP), and after

condenser. The components that will be modelled in this study are only the ejector and inter condenser. Figure 7 shows a schematic diagram of the GRS.

The ejector modelling process uses a system done in previous studies [31]. It begins by considering the need for motive steam or the main steam which is part of the steam going to the turbine. To obtain the steam requirement, a compression ratio with a specific value is used for a particular ejector, because, in the ejector the parameters are determined from the dimensions and operating area which are quite narrow. In addition, it is necessary to determine the entrainment ratio for the two fluids. The entrainment ratio formula [32] can be calculated using equation (5). After obtaining the entrainment ratio of each fluid, then the total air equivalent (TAE) is calculated by adding up the product of the mass flow rate and the entrainment ratio for the two fluids or can be seen in equation (6). NCG is a non-condensable gas, MS is the main vapor stream.

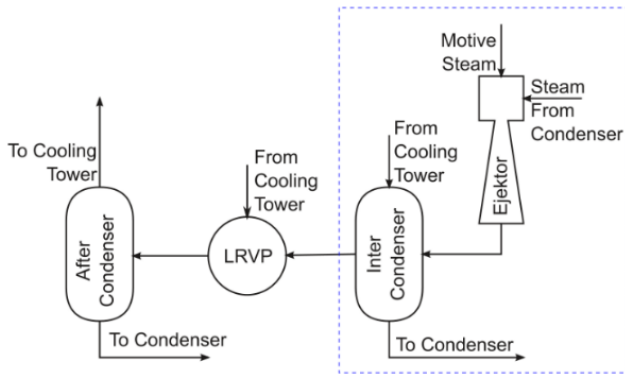


Figure 7. Gas removal system schematic diagram.

$$ER_f = \left[(5,73 \times 10^{-4} + 18,36) + \frac{2,01 \times M_f^{0,86}}{18,36 + M_f^{0,86}} \right] \quad (5)$$

$$TAE = \dot{m}_{NCG} \cdot E_{NCG} + \dot{m}_{MS} \cdot E_{MS}, \quad (6)$$

Furthermore, the calculation of the compression ratio and degree of expansion is carried out. The compression ratio (E) is the pressure ratio between the ejector outlet pressure and the non-condensable gas pressure or the pressure in the condenser. While the degree of expansion (K) is the ratio of the main vapor pressure to the pressure of the non-condensable gas or can be seen in equation (7).

$$E = \frac{P_{ejector}}{P_{NCG}} \quad (7)$$

Table 1. Model Validation to Actual Condition.

Parameter	Unit	Model Result	Actual Condition	Differences
P_{cond}	bar	0.1055	0.1050	+0.0005 (0.48%)
$T_{cond,out}$	°C	43.81	43.80	+0.01 (0.02%)
$T_{cooling}$	°C	25.53	25.5	+0.03 (0.11%)
$P_{ejector,suct}$	bar	0.099	0.098	+0,001 (0.11%)
$P_{ejector,out}$	bar	0.196	0.22	-0,024 (10.82%)
$\dot{m}_{ejector}$	kg/h	4980	4980	0
$T_{intercond, out}$	°C	43.33	45.50	-2.17 (4.76%)
$W_{turbine}$	MW	56.42	55	+1.42 (2.58%)

$$K = \frac{P_{MS}}{P_{NCG}} \quad (8)$$

The value of the compression ratio and the degree of expansion then matched on the graph (Figure 88) to get the ratio of air to steam so that the steam needed for the ejector will be obtained.

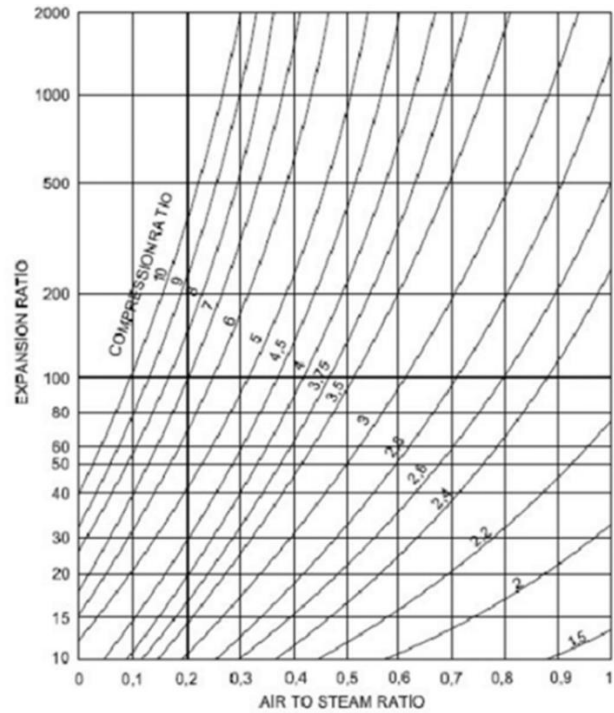


Figure 8. Air to steam ratio[32,33].

3.5 Geothermal Power Plant System

After all components can be modelled into interconnected system. The system modelling scheme is carried out in the following steps.

1. Enter the operating condition data of the entire system.
2. The P_{cond} is obtained from the model. The $T_{cond,out}$ value from the modelling results is used for input to the cooling tower components, as well as for the GRS system.
3. After the $T_{cooling}$ enters the cooling tower, the calculation of the cooling tower model is known to obtain input data for the condenser. This value is used as a convergence criterion for the iteration process so that the difference between the new and previous counts has a difference of 0.1%.

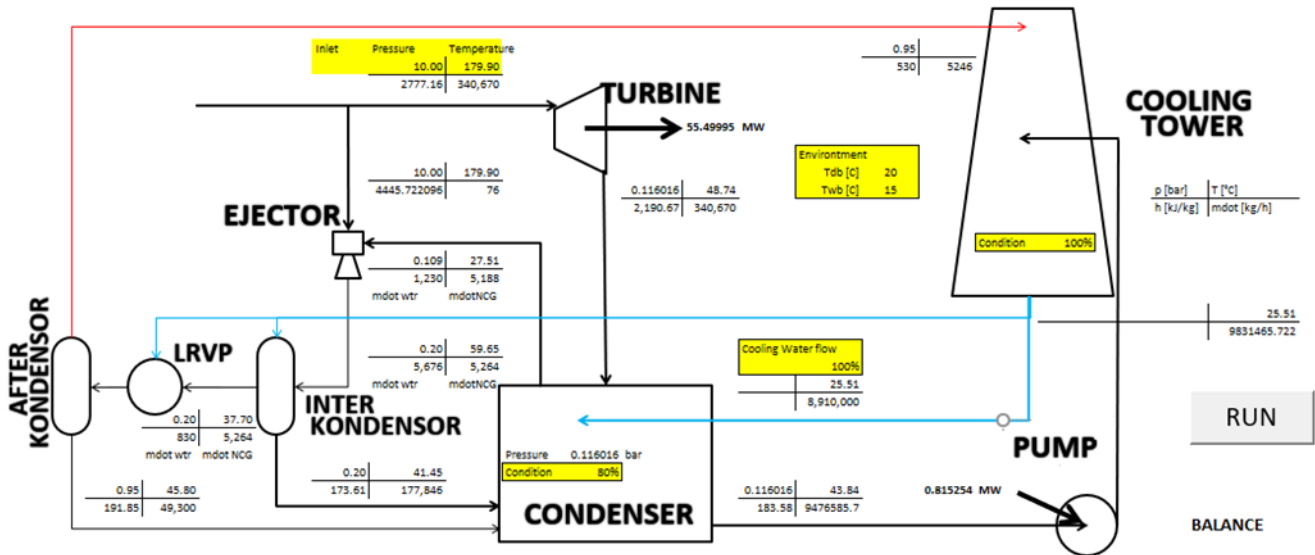


Figure 9. GPP model diagram.

4. Results and Discussion

Figure 9 show the GPP p model that used in this simulation. The simulations were carried out on existing modeling in Microsoft Excel coupled with Coolprop using three parameters; variations in condenser conditions represented by UA_{Cond} , variations in cooling tower capabilities represented by UA_{CT} , and variations in environmental conditions, especially variations in humidity represented by relative humidity (RH).

4.1 Model Validation

After each component has been successfully modelled and can be combined into a unified system that can iterate, the final schematic diagram of the analysis tool is obtained. The condition of the cooling tower and condenser is whether the condition of the two equipment can work properly or not. Wet and dry bulb represent the environmental condition. After the GPP system model can operate properly, validate the data from the modelling results and the actual operating conditions of the system as shown in Table 1.

In the modelling conditions, there is a significant difference in the ejector outlet pressure. This may be due to the difference between the modelling conditions that do not reflect the actual condition of the ejector itself. To get more precise conditions and according to actual conditions, it is necessary to conduct further research related to ejector modelling.

4.2 Results of Air Relative Humidity Variation

As we can see in Figure 10, shows the results of variations in relative humidity to turbine power and condenser pressure using a validated model. The increase in the relative humidity of the ambient air will increase the condenser pressure which decrease the turbine power produced. This shows that environmental conditions impact turbine performance, so environmental conditions need to be observed to know the changes that occur in the GPP system. GPP is very dependent on environmental conditions used to cool water by air from the surrounding environment. The cooled water is used to cool the water vapor in the condenser. Environmental conditions that are not by the initial design conditions will have an impact on turbine performance. This model shows by varying the relative humidity of the environmental air. The relative humidity parameter is used

because in the cooling tower, the relative humidity has an important factor in lowering the water temperature.

Figure 10 shows the impact of changes in environmental conditions on changes in condenser pressure that occur in the modelling in this study. The condenser pressure is related to the temperature of the cooling water entering the condenser to cool the water vapor. When the ability of the ambient air to cool the cooling water in the cooling tower decreases, indicated by an increase in relative humidity, the temperature of the cooling water entering the condenser will increase. This condition causes an increase the pressure in the condenser. This condenser pressure increment will decrease the turbine power generated. This is because the pressure influence the expansion process of water vapor in the turbine. If the condenser pressure increases, the steam expansion process will not be optimal and reduce the turbine power. Increasing the relative humidity of the ambient air by up to 90% will reduce turbine power by up to 2.26%. Jian li et al shows that the increase of air relative humidity will decrease the power generated in geothermal power plant. The power generated in geothermal power plant sensitive to the ambient condition in the view of relative variation [34].

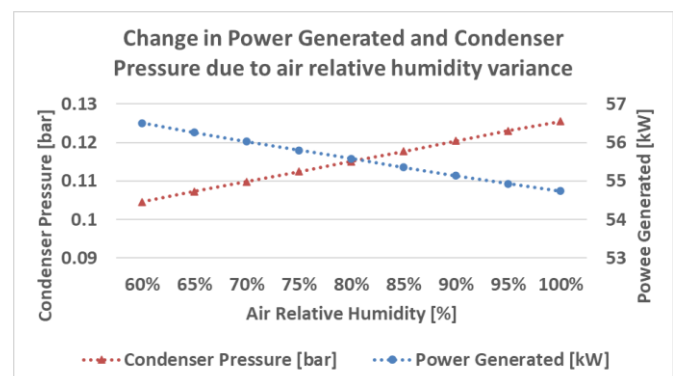


Figure 10. Change in power generated and condenser pressure due to air relative humidity variance (Figure is in color in the on-line version of the paper).

4.3 Result of Condition Cooling Tower Variation

The next simulation is to change condition on the cooling tower. The value of UA_{CT} physically can be likened to the condition of the cooling tower. How well the cooling tower can cool the water that will later be used in the condenser. This simulation does not consider changes that occur in the

environment. Changes condition can be caused by a decrease in the number of working nozzles, and the presence of dirt in the packing section.

The parameter to be reviewed first is the change that occurs in the condenser pressure. Figure 11 illustrates the effect of changing the cooling tower condition on the condenser pressure. As with the worse condition of cooling tower will increase the pressure in the condenser. Even if the condition of the cooling tower decreases to 60%, the condenser pressure is close to the operating limit. If the cooling tower condition continues to be lowered until the condenser working pressure limit is reached, which is 0.015 bar, then the cooling tower condition limit is 56%. In this condition, the condenser will turn off.

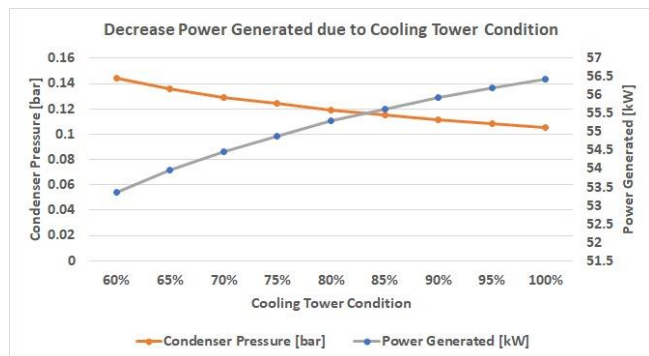


Figure 11. The effect of cooling tower condition to the change of condenser pressure and power generation (Figure is in color in the on-line version of the paper).

Meanwhile the blue line show in Figure 11 shows the relationship between changes in the cooling tower condition to the turbine power generated by this generator system model. The turbine power produced will decrease as the condition of cooling tower worsened.

4.4 Result of Condition Condenser Variation

The amount of UA_{COND} on the condenser represents the condition of the condenser. Physically, UA_{COND} can be interpreted from how good the condition of the condenser is. In this modeling, UA_{COND} is used during the process of condensing the steam into water, so several things that will affect the value of UA_{COND} include the condition of the nozzles on the condenser used to mist the cooling water, then the amount of non-condensable gas that changes. Both can reduce the ability of the condenser to condense steam from the turbine. The first parameter to be reviewed is the impact of changes in condenser pressure by changes in the condenser condition as shown in Figure 12. In the Figure 12, as we can see as the condition of the condenser decreases from 100% to 60%, the condenser pressure will continue to increase. This means that the vacuum level in the condenser decreases.

Meanwhile in the same of Figure 12, the parameter that is reviewed after the water condition in the condenser is the turbine power that is generated when there is a decrease in the condenser condition is the power generated. Turbine power is the most visible parameter compared to other parameters because it is the output that will be used directly. The increase in condenser pressure will result around the interior of the cycle being reduced so that the total power generated will also decrease. In this study, decreasing the quality of the condenser up to 60% will reduce the turbine power by 4.63%.

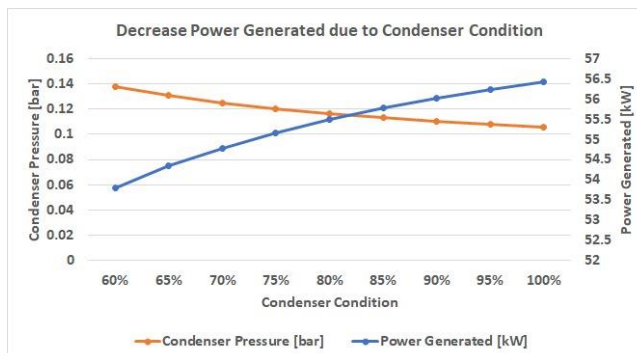


Figure 12. The effect of condenser condition to the change of condenser pressure and power generation (Figure is in color in the on-line version of the paper).

5. Conclusion

The results obtained in this study include:

- The modeling of the geothermal power plant system can be modeled using Microsoft Excel software and has been validated using the operating conditions of the geothermal power plant system owned by PT. Indonesia Power in Mount Darajat. This model can be used as quick help tools to know the condition and effect in any GPP that using vapor as working fluid.
- Changes in the condition of condenser and cooling tower and environmental condition have direct impact to the turbine performance. With varying the condition of cooling tower, condenser, and environmental decrease the turbine power generated 5.41%, 4.63%, and 2.26% respectively. The decrease turbine power generated by changes in environmental condition fit with Jian li research results.
- It needs further research and modelling to get better model and understanding in NCG extraction system.

Nomenclature

C_p	Specific heat	(kJ/kg.K)
E	compression ratio	(-)
ER	Entrainment ratio	(-)
h	Enthalpy specific	(kJ/kg)
K	degree of expansion	(-)
Mr	fluids mass molar relative	(g/mol)
\dot{m}	mass flow rate	(kg/h)
\dot{m}_a	mass flow rate of ambient	(kg/h)
\dot{m}_b	mass flow rate of blowdown	(kg/h)
\dot{m}_d	mass flow rate of air	(kg/h)
P	Pressure	(bar)
T	Temperature	(°C)
UA	Total coefficient of heat transfer	(W/m ² .K)
\dot{W}	Work	(kW)
x	fraction	(-)
η	Efficiency	(%)

Subscripts

a	ambient
b	blowdown
$cond$	condenser
$cond,out$	Condenser out
$Cooling$	Cooling
CT	Cooling tower
$ejector,suct$	Suction of ejector
$intercond,out$	Outlet of inter-condenser
cw	Cooling water
d	air

<i>f</i>	fluids
<i>ms</i>	Motive steam
<i>turbine</i>	turbine

Abbreviations

<i>BCV</i>	Ball check valve
<i>CP</i>	Cooling pump
<i>CWP</i>	Cooling water pump
<i>CS</i>	Cyclone separator
<i>EBTKE</i>	Energy and Mineral Resources directorate in the field of Renewable Energy Conservation
<i>GPP</i>	Geothermal power plant
<i>GRS</i>	Gas remover system
<i>LMTD</i>	Log mean temperature difference
<i>LRVP</i>	Liquid ring vacuum pump
<i>MR</i>	Mist remover
<i>MTOE</i>	Mega tonnes of oil equivalent
<i>MV</i>	Main vapour steam
<i>NCG</i>	Non-condensable gas
<i>ORC</i>	Organic Rankine cycle
<i>PC</i>	Pump circulation
<i>PLN</i>	Perusahaan listrik negara
<i>RH</i>	Relative humidity
<i>SE/C</i>	Ejector system
<i>TAE</i>	Total air equivalent
<i>WV</i>	Water valve

Author contribution statement

KFAS as main contributor write the manuscript, developing the model program in excel, collecting the data. DIP write the introduction section, final review and correspondences. WA is as supervisor for this research and conceive the research idea.

References:

- [1] Perusahaan Listrik Negara, *Rencana Usaha Penyediaan Tenaga Listrik (RUPTL) 2021 - 2030 PT PLN (Persero)* [online]. Available: <https://web.pln.co.id/statics/uploads/2021/10/ruptl-2021-2030.pdf> (accessed Des, 8, 2021).
- [2] ESDM, *Terus Dorong Percepatan Pengembangan EBT, Pemerintah Siapkan PLN Khusus EBT* [online]. 2016. available: <https://ebtke.esdm.go.id/post/2016/01/07/1075/terus.dorong.percepatan.pengembangan.ebt.pemerintah.siapkan.pln.khusus.ebt> (accessed Des, 8, 2021).
- [3] Badan Pengkajian dan Penerapan Teknologi, *Outlook Energi Indonesia 2014; Pengembangan Energi untuk Mendukung Program Substitusi BBM*. Jakarta: Pusat Teknologi Pengembangan Sumberdaya Energi, 2014.
- [4] M. I. Kömürçü and A. Akpınar, "Importance of geothermal energy and its environmental effects in Turkey," *Renew. Energy*, vol. 34, no. 6, pp. 1611–1615, 2009.
- [5] Dirjen EBTKE, *Statistik EBTKE 2016*. Jakarta: EBTKE, 2016.
- [6] A. Hepbasli, "A review on energetic, exergetic and exergoeconomic aspects of geothermal district heating systems (GDHSs)," *Energy Convers. Manag.*, vol. 51, no. 10, pp. 2041–2061, 2010.
- [7] A. Hepbasli and C. Canakci, "Geothermal district heating

- applications in Turkey: A case study of Izmir-Balcova," *Energy Convers. Manag.*, vol. 44, no. 8, pp. 1285–1301, 2003.
- [8] K. Popovski and S. P. Vasilevska, "Prospects and problems for geothermal use in agriculture in Europe," *Geothermics*, vol. 32, no. 4, pp. 545–555, 2003.
- [9] B. Tomaszewska *et al.*, "Utilization of renewable energy sources in desalination of geothermal water for agriculture," *Desalination*, vol. 513, 2021.
- [10] P. Jiang, X. Li, R. Xu, and F. Zhang, "Heat extraction of novel underground well pattern systems for geothermal energy exploitation," *Renew. Energy*, vol. 90, no. 2016, pp. 83–94, 2016.
- [11] Y. Yuan, T. Xu, Z. Jiang, and B. Feng, "Prospects of power generation from the deep fractured geothermal reservoir using a novel vertical well system in the Yangbajing geothermal field, China," *Energy Reports*, vol. 7, pp. 4733–4746, Nov. 2021.
- [12] L. Zhang, S. Chen, and C. Zhang, "Geothermal power generation in China: Status and prospects," *Energy Sci. Eng.*, vol. 7, no. 5, pp. 1428–1450, 2019.
- [13] Massachusetts Institute of Technology, "The Future of Geothermal Energy," 2006.
- [14] M. A. Ehyaei, A. Ahmadi, M. A. Rosen, and A. Davarpanah, "Thermodynamic optimization of a geothermal power plant with a genetic algorithm in two stages," *Processes*, vol. 8, no. 10, pp. 1–16, 2020.
- [15] E. E. Michaelides and D. N. Michaelides, "The effect of ambient temperature fluctuation on the performance of geothermal power plants," *Int. J. Exergy*, vol. 8, no. 1, pp. 86–98, 2011.
- [16] M. Kahraman, A. B. Olcay, and E. Sorgüven, "Thermodynamic and thermoeconomic analysis of a 21 MW binary type air-cooled geothermal power plant and determination of the effect of ambient temperature variation on the plant performance," *Energy Convers. Manag.*, vol. 192, no. April, pp. 308–320, 2019.
- [17] M. I. Sohel, M. Sellier, L. J. Brackney, and S. Krumdieck, "An iterative method for modelling the air-cooled organic Rankine cycle geothermal power plant," *Int. J. Energy Res.*, vol. 35, no. 5, pp. 436–448, Apr. 2011.
- [18] B. Rudiyanto *et al.*, "Preliminary analysis of dry-steam geothermal power plant by employing exergy assessment: Case study in Kamojang geothermal power plant, Indonesia," *Case Stud. Therm. Eng.*, vol. 10, pp. 292–301, 2017.
- [19] M. Aneke, B. Agnew, and C. Underwood, "Performance analysis of the Chena binary geothermal power plant," *Appl. Therm. Eng.*, vol. 31, no. 10, pp. 1825–1832, 2011.
- [20] H. Ghasemi, M. Paci, A. Tizzanini, and A. Mitsos, "Modeling and optimization of a binary geothermal power plant," *Energy*, vol. 50, no. 1, pp. 412–428, 2013.
- [21] X. Zhang, M. He, and Y. Zhang, "A review of research on the Kalina cycle," *Renew. Sustain. Energy Rev.*, vol. 16, no. 7, pp. 5309–5318, 2012.

- [22] H. Li, D. Hu, M. Wang, and Y. Dai, "Off-design performance analysis of Kalina cycle for low temperature geothermal source," *Appl. Therm. Eng.*, vol. 107, pp. 728–737, 2016.
- [23] D. I. Permana, D. Rusirawan, and I. Farkas, "Waste heat recovery of tura geothermal excess steam using organic rankine cycle," *Int. J. Thermodyn.*, vol. 24, no. 4, pp. 32–40, 2021.
- [24] K. Li, C. Liu, S. Jiang, and Y. Chen, "Review on hybrid geothermal and solar power systems," *J. Clean. Prod.*, vol. 250, 2020.
- [25] A. Dagdas, M. T. Akkoyunlu, and T. Basaran, "Performance Analysis of Supercritical Binary Geothermal Power Plants," *Adv. Mech. Eng.*, vol. 7, no. 1, 2015.
- [26] H. Moon and S. J. Zarrouk, "Efficiency of Geothermal Power Plants: a Worldwide Review," *Geothermics*, vol. 51, no. November 2012, pp. 142–153, 2014.
- [27] B. Ciapała, J. Jurasz, M. Janowski, and B. Kępińska, "Climate factors influencing effective use of geothermal resources in SE Poland: the Lublin trough," *Geotherm. Energy*, vol. 9, no. 1, pp. 1–16, 2021.
- [28] R. DiPippo, *Geothermal Power Plants; Principles, Applications, Case Studies and Environmental Impact*, 2nd ed. New York: McGraw-Hill, Inc., 2007.
- [29] P. K. Nag, *Power Plant Engineering*, 3rd ed., vol. 1. New Delhi: McGraw-Hill, Inc., 2008.
- [30] M. H. Dickson and M. Fanelli, "What is geothermal energy? International Geothermal Association (IGA): [htt:iga.igg.cnr.it/geo/geoenergy.php](http://iga.igg.cnr.it/geo/geoenergy.php)," pp. 1–33, 2004.
- [31] M. Hasan, "Analisi Kinerja Ejektor Terhadap Kenaikan Persentase Gas Tak Terkondensasi Unit 1 dan 2 PLTP Gunung Salak," Insitut Teknologi Bandung, 2007.
- [32] N. Y. Özcan and N. Y. Ozcan, "Modeling, Simulation and Optimization of Flashed-Steam Geothermal Power Plants from the Point of View of Noncondensable Gas Removal Systems," Izmir Institute of Technology, 2010.
- [33] Geothermal Institute, "Gas Extraction System," in *Course note of Geothermal Institute*, Auckland University, 1996, p. 75.
- [34] J. Li, Z. Yang, Z. Yu, J. Shen, and Y. Duan, "Influences of climatic environment on the geothermal power generation potential," *Energy Convers. Manag.*, vol. 268, no. April, p. 115980, 2022.